

Synthesis of an oligonucleotide-derivatized amphilipol and its use to trap and immobilize membrane proteins

Christel Le Bon¹, Eduardo Antonio Della Pia², Fabrice Giusti¹, Noémie Lloret², Manuela Zoonens¹, Karen L. Martinez² and Jean-Luc Popot^{1,*}

¹UMR 7099, Centre National de la Recherche Scientifique/Université Paris-7, Institut de Biologie Physico-Chimique (FRC 550), 13 rue Pierre et Marie Curie, F-75005 Paris, France and ²Bio-Nanotechnology and Nanomedicine Laboratory, Department of Chemistry and Nano-Science Center, University of Copenhagen, Universitetsparken 5, DK-2100 Copenhagen, Denmark

Received January 9, 2014; Revised February 25, 2014; Accepted March 13, 2014

ABSTRACT

Amphilipols (APols) are specially designed amphiphilic polymers that stabilize membrane proteins (MPs) in aqueous solutions in the absence of detergent. A8–35, a polyacrylate-based APol, has been grafted with an oligodeoxynucleotide (ODN). The synthesis, purification and properties of the resulting ‘OligAPol’ have been investigated. Grafting was performed by reacting an ODN carrying an amine-terminated arm with the carboxylates of A8–35. The use of OligAPol for trapping MPs and immobilizing them onto solid supports was tested using bacteriorhodopsin (BR) and the transmembrane domain of *Escherichia coli* outer membrane protein A (tOmpA) as model proteins. BR and OligAPol form water-soluble complexes in which BR remains in its native conformation. Hybridization of the ODN arm with a complementary ODN was not hindered by the assembly of OligAPol into particles, nor by its association with BR. BR/OligAPol and tOmpA/OligAPol complexes could be immobilized onto either magnetic beads or gold nanoparticles grafted with the complementary ODN, as shown by spectroscopic measurements, fluorescence microscopy and the binding of anti-BR and anti-tOmpA antibodies. OligAPols provide a novel, highly versatile approach to tagging MPs, without modifying them chemically nor genetically, for specific, reversible and targetable immobilization, e.g. for nanoscale applications.

INTRODUCTION

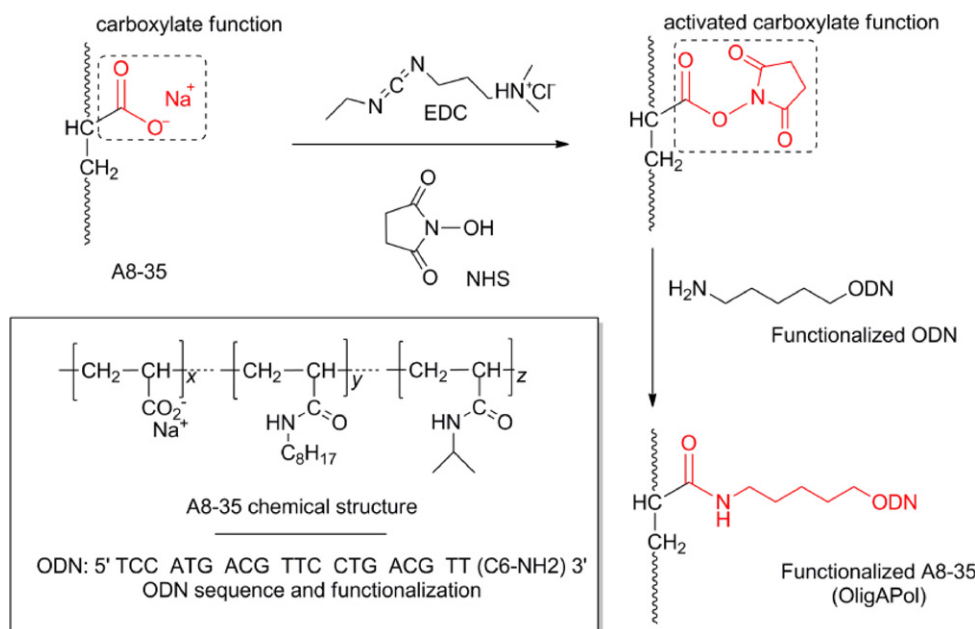
Amphilipols (APols) are amphiphilic polymers that, when substituted to detergents, stabilize membrane proteins (MPs) in aqueous solutions (1,2). Their rich chemistry lends

itself to a large variety of applications, among which is the indirect functionalization of the MPs they bind to (3–5). The most thoroughly studied APol to date, A8–35 (6), comprises a short polyacrylate backbone [\sim 35 acrylate residues; see (7)] randomly grafted with octylamine and isopropylamine side chains (Inset of Scheme 1). The average molecular mass of A8–35, which varies slightly depending on that of the polyacrylate used for the synthesis, is \sim 4.3 kDa (7). In aqueous solutions, A8–35 self-organizes (8,9) into small, globular, well-defined particles, whose average mass is \sim 40 kDa (10), and which, therefore, comprise on average \sim 9–10 molecules. When an MP in detergent solution is supplemented with APols and the detergent removed, water-soluble MP/APol complexes form, in which the APol specifically adsorbs onto the hydrophobic transmembrane surface of the protein [reviewed in (2)]. Although it is non-covalent, the association of APols with MPs, because it involves multiple hydrophobic contact points, is essentially irreversible even under conditions of extreme dilution, unless APols are displaced by an excess of another surfactant (3,11,12). Complexation of an MP with a functionalized APol will therefore result in a stable functionalized complex. In the present work, this property has been exploited to develop a general approach to immobilizing MPs onto solid supports via an oligodeoxynucleotide (ODN)-tagged APol.

The chemistry of APols offers a wide range of resources, which permit to tailor them to specific biophysical or biochemical applications [reviewed in (5)]. Thus, A8–35 has been deuterated (13) and perdeuterated (7) in view of applications in nuclear magnetic resonance (NMR) [reviewed in (14)], small angle neutron scattering or analytical ultracentrifugation [see, e.g. (15)]. APols labeled with various fluorophores (FAPols) have been used for studying the kinetics of exchange of A8–35 at the surface of MPs (3) and its critical association constant (9).

Tagged APols can be used for trapping and immobilizing MPs onto solid supports. This application was first demonstrated using biotinylated A8–35 (BAPol). Various

*To whom correspondence should be addressed. Email: jean-luc.popot@ibpc.fr



Scheme 1. Reaction scheme for OligAPol synthesis. The formation of an activated carboxylate moiety by reaction with EDC and NHS is followed by grafting of the amine-functionalized oligonucleotide (ODN) to form an amide bond. Inset: chemical structure of A8-35 [$x \approx 35\%$, $y \approx 25\%$, $z \approx 40\%$; from (6)] and sequence of ODN CpG-1826.

MP/BAPol complexes were immobilized onto streptavidin-coated beads or chips, and the interaction of antibodies and pharmacological ligands with the proteins evidenced by either surface plasmon resonance or fluorescence microscopy (4,16,17). Four of the many advantages of using tagged APols to indirectly tag MPs are (i) that any MP can be immobilized, using a single tagged APol, without having undergone any genetic or chemical modification, (ii) that trapping in most cases stabilizes biochemically the protein, (iii) that ligand binding can be measured in aqueous, detergent-free solutions and (iv) that a large variety of tags can in principle be used without having to develop often complex or hazardous ways to attach them covalently to the target MPs. Key features include the specificity of the attachment to the support, its stability and its reversibility, the latter being particularly important when working with costly supports that have to be regenerated. Because biotin-mediated anchoring is essentially irreversible, exploring alternative attachment modes is desirable.

We examine here the possibility of functionalizing A8-35 with ODNs. The reversible immobilization of MPs via an ODN tag presents major assets for the regeneration and reconfiguration of biosensors and biochip surfaces. In addition, ODNs offer rich possibilities of modulating the stability and specificity of the attachment, by playing on their length and sequence, and they lend themselves well to multiplexing. They provide a chemically mild method for the site-selective immobilization of multiple MPs onto solid supports: traditional, well-established deoxyribonucleic acid (DNA) microarrays could be easily adapted as immobilization platforms. Previous studies have demonstrated sequence-specific and site-selective immobilization of semi-synthetic protein-ODN conjugates onto surfaces modified with complementary nucleotide sequences (18,19). How-

ever, these methods require protein engineering or chemical modification and cannot be easily adapted to MPs, which tend to be fragile and hard to handle. An alternative strategy is to first reconstitute the target MP in liposomes containing a cholesterol-modified ODN and then bind the proteoliposomes onto surfaces modified with the complementary ODN (cODN) (20). Reconstitution of MPs, however, is a delicate, protein-specific process, and its optimization is time-consuming.

In this article, we first describe a route for synthesizing and purifying ODN-grafted A8-35. The ability of the resulting ‘OligAPol’ to trap and anchor MPs onto surfaces carrying the cODN is demonstrated using two different types of solid supports, magnetic beads and gold nanoparticles (Au NPs). In both cases, adsorption is specifically mediated by formation of the DNA duplex. Magnetic beads give access to adsorption yields, Au NPs to the homogeneity and reversibility of the adsorption.

MATERIALS AND METHODS

Materials

APol A8-35 was synthesized and characterized according to the procedure described in (10,13), FAPol_{NBD} according to that described in (3). ODNs were purchased from Trilink or Alpha DNA. Their characteristics are listed in Table 1. 1-Ethyl-3-[3-dimethylaminopropyl]carbodiimide hydrochloride (EDC) was from Alpha Aesar, *N*-hydroxysuccinimide (NHS) and sodium cyanoborohydride (NaCNBH₃) from Sigma Chemicals, Bio-Beads SM-2 from Biorad and *n*-octyl- β -D-thioglucopyranoside (OTG) from Anatrace. Aldehyde-activated magnetic beads (1- μm diameter) were from Bioclone. The succinimidyl ester of Alexa Fluor 647 was from Invitrogen. Perdeuterated NMR solvents were

from VWR. Glass cover-slips (25-mm diameter, 0.17 ± 0.01 mm thick) were purchased from Hounisens Laboratoriumstyr, 100-nm Au NPs and poly-L-lysine (PLL) from Sigma and 2-[methoxy(polyethyleneoxy)propyl]trimethoxysilane, tech-90 (PEG silane) from Gelest.

Buffers

Phosphate buffer: 100-mM NaCl, 20-mM sodium phosphate, pH 7.0. Standard chromatography buffer: 100-mM NaCl, 20-mM Tris/HCl, pH 8.0. For experiments with magnetic beads, coupling buffer was 100-mM sodium phosphate, pH 7.0; washing buffer: 1-M NaCl; hybridization buffer: 300-mM NaCl, 30-mM sodium citrate, pH 7.4. For immobilization on Au NPs, TE buffer was 10-mM Tris, pH 8.0, 1-mM ethylenediaminetetraacetic acid (EDTA); PPB was 10-mM potassium phosphate buffer, pH 7.2; PPB-T20 was PPB + 0.001% Tween 20.

Methods

OligAPol synthesis and purification. Stock solutions of A8–35 and ODN prepared in 0.4-M NaCl were stored at 4°C; NHS and EDC were dissolved extemporaneously in 0.1-M phosphate buffer, pH 6.8. 3 ml of a 20.7-g/l A8–35 solution (~14.4 µmol polymer or ~176-µmol free carboxylate functions) and 1.5 ml of a 15-g/l ODN solution (~3.4 µmol) were supplemented with 0.2 ml of a 600-g/l EDC and 114-g/l NHS solution (molar ratios 4:1 and 1:1, respectively, with respect to free carboxylate functions). The solution was kept under stirring for 48 h and the reaction monitored by fast protein (or fast performance) liquid chromatography (FPLC; see below) with the injection of 25-µl aliquots diluted to 300 µl with chromatography buffer. The reaction medium (~4.5 ml) was diluted in 50-ml phosphate buffer, pH 3.25, inducing precipitation of the polymer. The pellet was recovered after a 5000-rpm centrifugation at 4°C during 15 min and resolubilized in 4.5 ml of phosphate buffer, pH 8. The cycle of precipitation/solubilization was repeated twice and followed by preparative size exclusion chromatography (SEC) on the FPLC system. The collected fractions were concentrated under 2 atm in a stirred Millipore Alphacell with 10-kDa porosity to reduce the volume to 50 ml. The solution was filtered through a 0.2-µm syringe filter, dialyzed against water purified on a A10 Advantage Millipore System (mQ water) using a Spectra/Por dialysis membrane (cut off 6–8 kDa) for at least 2 h, and finally freeze-dried, yielding 50 mg of purified OligAPol (yield relative to A8–35: ~60%). [The yield of grafting never exceeded one ODN per two particles. Repulsive interactions between the two negatively charged partners (ODN and A8–35), as well as the limited solubility of intermediates, may limit the extent of derivatization. Reacting EDC with carboxylates to form first an *O*-acylurea intermediate, which evolves into an amine-reactive NHS ester in the presence of NHS, reduces the number of free carboxylates that confer to A8–35 its high solubility (10,13). Some of these groups subsequently become grafted with the highly hydrophilic ODN, but the majority of them do not, leading to a global increase of hydrophobicity until the ester is hydrolyzed to regenerate the carboxylate. Since the balance of hydrophilic and hy-

drophobic groups in A8–35 is delicately poised (10,13), this can lead to aggregation.]

FAPol_{AF647} synthesis. The detailed synthesis protocol of the fluorescent APol FAPol_{AF647} is described elsewhere (21). Briefly, it consists in reacting the amine moiety of the ‘universal’ APol [A8–35 grafted with a spacer arm carrying an amine function; (3)] with the succinimidyl ester function of a functionalized Alexa Fluor 647 dye. The grafting ratio is ~3 fluorophores per 1000 PAA units. Each FAPol_{AF647} particle, which comprises ~325 units, carries therefore ca. one fluorophore. FAPol_{AF647} presents an absorption maximum at 651 nm and an emission maximum at 668 nm (21).

Size exclusion chromatography. SEC was performed at room temperature (RT) on an Äkta Purifier 10 FPLC system (GE Healthcare). Detection was performed at three wavelengths: 220, 260 and either 280 or 554 nm. For analysis purpose, the system was equipped with a Superose 12 10/300 GL column calibrated according to (22). For purification purpose, it was equipped with an XK 26/100 column filled with Superose 12 prep grade. Pre-equilibration of the columns was performed with either chromatography or phosphate buffer. The elution flow rate was set at 0.5 ml/min. Peak characteristics (elution volume, area and width at half-height) were determined using the Unicorn software.

For SEC characterization of the purified OligAPol, stock solutions of ODN (5 g/l, i.e. ~0.76 mM), OligAPol (98 g/l) and A8–35 (116 g/l, i.e. ~27 mM) were prepared in mQ water and separately diluted (by 10× for the ODN and by 20× for the two APols) in chromatography buffer prior to injection onto the Superose 12 10/300 GL column.

NMR and optical spectroscopy analyses, imaging. ¹H and ¹³C NMR spectroscopy of A8–35 was performed on a Bruker Avance 400-MHz NMR spectrometer at RT in perdeuterated methanol (CD₃OD), as previously described (13). ¹H NMR spectroscopy of OligAPol and ODN was realized in a mixture of perdeuterated methanol (CD₃OD) and water (D₂O). Examining the chemical composition of the purified OligAPol by ¹H NMR spectroscopy was poorly informative, because most of the ODN signals overlap with those of A8–35 (not shown). Aromatic protons (7–9 ppm) were only weakly detected and their signal could not be integrated with acceptable accuracy. As regards the octylamine and isopropylamine grafting ratios, however, they cannot have been affected, considering the OligAPol synthesis strategy, and are necessarily the same for one given OligAPol and its A8–35 precursor.

Optical spectroscopy measurements were carried out on an HP-8453 UV-VIS spectrometer (Agilent Technologies).

Imaging of Au NPs was performed using a Leica DM5500 B upright wide-field microscope equipped with epifluorescence optics and a ×63 water immersion objective. Images were recorded using the following settings of the excitation and emission filters: (i) excitation 470/40 nm—central wavelength and band-width of the filter, emission 525/50 nm for the anti-bacteriorhodopsin (BR) antibody labeled with Alexa Fluor 488; (ii) excitation 531/40 nm, emission 593/40 nm for the ODN labeled with a

Table 1. ODNs used in the present work, with their sequence, their mass, the backbone type and, if applicable, the type(s) of functionalization used

Name	Sequence	Mass (Da)	Backbone	Functionalization
ODN cODN	5' TCC ATG ACG TTC CTG A'CG TT 3'	6559.3	PS	C6-amino linker in 3'
	3' AGG TAC TGC AAG GAC TCG 5'	6016.8	PS	C6-amino linker in 3'
			PS	thiol in 3'
polyC polyT	5' CCC CCC CCC CCC CCC CCC 3'	5339.3	PS	thiol in 3'
	5' TTT TTT TTT TTT 3'	3588.4	PO	None

ODN stands for the CpG-1826 ODN, cODN for its complementary sequence, polyC for polycytosine and polyT for polythymine. The backbone bond linking the nucleotides can be either a phosphorothioate (PS) or a phosphodiester (PO) function.

Cy3 dye; (iii) excitation 620/60 nm, emission 700/75 nm for FAPolAF₆₄₇ and anti-tOmpA labeled with Alexa Fluor 647. All fluorescence microscopy images presented here are false-color images.

Purple membrane purification and preparation of BR/APol complexes. Purple membrane (PM) purification was carried out as described in (15). PM in phosphate buffer at a BR concentration close to 6 g/l was solubilized with 100-mM OTG (cmc ≈ 9 mM) for 40 h in the dark at 6°C and ultracentrifuged at 200 000 × g for 20 min at 6°C in a TL 100 ultracentrifuge (Beckman Coulter). The supernatant was diluted from 100-mM to 18-mM OTG with phosphate buffer. The concentration of solubilized BR was calculated from its absorbance at 554 nm using $\epsilon_{554} = 43\,000\text{ M}^{-1}\text{ cm}^{-1}$.

The protocol for the preparation of BR/APol complexes was adapted from (15). It comprises the following steps : (i) formation of a ternary BR/OTG/APol complex by adding aliquots of a 100-g/l APol stock solution to 300 µl of solubilized BR; the final BR/APol mass ratio was varied from 1:2 to 1:10; (ii) 20-min incubation on a rotating wheel at 4°C in the dark; (iii) removal of the detergent by adsorption onto polystyrene beads (Bio-Beads SM-2) at a 10:1 beads/OTG mass ratio, during overnight (ON) incubation on a wheel at 4°C in the dark; (iv) ultracentrifugation at 100 000 × g at 4°C for 20 min to remove aggregated material. Ultraviolet (UV)-visible absorption spectra were recorded before and after ultracentrifugation to quantify the percentage of BR kept soluble by the APol. Control samples included BR in 18-mM OTG (no APol and no beads added; positive control) and BR depleted of OTG in the absence of APol (negative control).

Purification of tOmpA and preparation of tOmpA/APol complexes. The transmembrane domain of outer membrane protein A from *Escherichia coli* (tOmpA) was produced as described in (23). Briefly, tOmpA was overexpressed in *E. coli* BL21(DE3). After cell lysis, inclusion bodies were harvested by centrifugation at 4300 × g and washed with 2% Triton X-100 before being solubilized in 20-mM Tris/HCl, pH 8.0, 8-M urea. Refolding was carried out by dialysis in the presence of tetraethylene glycol monooctyl ether (C₈E₄) and the protein purified by ion exchange chromatography on a 5-ml HiTrap Q HP column (GE Healthcare) connected to an Äkta Purifier device. The equilibration buffer was 20-mM Tris/HCl, pH 8.0, 19.6-mM C₈E₄. The elution buffer contained, in addition, 1-M

NaCl. The protocol for the preparation of tOmpA/APol complexes was similar to that of BR/APol complexes, but for the MP/A8–35 w/w ratio, which was 1:4 (3).

cODN grafting onto magnetic beads. The protocol was adapted from that given by Bioclone. Two-milligram aliquots of aldehyde-activated magnetic beads were rehydrated, washed three times with 500 µl of coupling buffer and supplemented with a solution of functionalized cODN (75 µl of cODN at 2 g/l diluted with 275 µl of coupling buffer) plus 10 µl of NaCNBH₃ (250 mM in 1-M NaOH, prepared extemporaneously in a chemistry fume hood due to its toxicity). After ON incubation on a wheel at RT, the coupling efficiency was estimated from the cODN concentration remaining in the supernatant, determined by UV spectrophotometry. Beads were then washed three times with 500 µl of washing buffer. Non-specific interactions were blocked by ON incubation at RT on a wheel in a solution of polythymine (25 µl of polyT at 2 g/l diluted with 275 µl of hybridization buffer). Beads were washed three times with 500 µl of hybridization buffer before use.

Immobilization onto cODN-grafted magnetic beads. Two milligrams of beads in 275-µl hybridization buffer were supplemented with either (i) 25 µl of 2-g/l ODN solution, (ii) 25 µl of 2-g/l polyT solution, (iii) 25 µl of 10-g/l A8–35 solution or (iv) 25 µl of 10-g/l OligAPol solution. After 20-min incubation at RT on a rotating wheel, supernatants were separated from the beads using a magnet and analyzed by UV-visible spectrometry and SEC. For immobilizing BR/OligAPol complexes, the protocol was modified as follows: 100 µl of complexes formed at 1:7.5 BR/OligAPol mass ratio (in trapping buffer) were diluted with 100-µl MQ water. The final concentrations of BR and OligAPol were, respectively, 0.178 and 1.336 g/l. The solution was incubated with 2 mg of cODN-grafted beads on a rotating wheel in the dark at 4°C for 2 × ~15 h at 4°C, with a renewal of the beads at mid-time. It is notable that equilibrium depletion was reached more slowly with the BR/OligAPol complexes than with the other samples, and it required the addition of more beads. It seems probable that, because of their larger size and the lower temperature, MP/OligAPol complexes diffuse more slowly into the beads and do not have access to the same proportion of bead-attached cODN as free ODN or OligAPol particles do.

Immobilization of BR trapped in OligAPol onto Au NPs. In order to directly visualize the anchoring of BR trapped in

OligAPol onto gold surfaces, 100-nm diameter Au NPs were deposited onto glass cover-slips modified as follows. The glass surface was cleaned for 10 s with acetone, methanol and ethanol and with plasma etching for 200 s. The glass slide was then placed on a flat and clean surface and immersed successively in 50 ml of ethanol, 40- μ l concentrated HCl (37.2%, 12.1 M), 100- μ l PEG silane and 100 μ l of 1-g/1 PLL solution for 60 min (the PLL solution was sonicated for 15 min prior to incubation). The glass slide was washed with ethanol and deionized water for 10 s, then incubated for 30 min at 75°C. The slide surface was covered with a 20- μ l solution of Au NPs (diluted in deionized H₂O to a final concentration of 3.8×10^8 particles per ml) for 30 min. The slide was then rinsed for 10 s with a stream of deionized H₂O and dried for 60 s under a gentle stream of N₂.

After deposition of Au NPs, the glass slide was incubated for 1 h with 100 μ l of 2- μ M cODN, functionalized with a thiol tag, diluted in 10-mM Tris pH 8.0, 1-mM EDTA (TE buffer) and washed for 10 s with TE buffer. In order to assess the accessibility of the cODN on the Au NP surface, the glass slide was incubated for 2 h with 100 μ l of 1- μ M ODN functionalized with a Cy3 fluorescent tag. In order to investigate the immobilization of MPs onto modified Au NPs, it was incubated for 2 h with 100 μ l of 1- μ M BR or tOmpA trapped in a 1:1 OligAPol/FAPol_{AF647} mixture. Before imaging, the glass surface was incubated for 10 min in PPB-T20 with shaking and washed three times with 10-ml PPB in order to remove non-specifically bound proteins.

In order to demonstrate the presence of the MPs at the surface of the Au NPs, NPs functionalized with the thiolated cODN were first incubated for 2 h either with 1- μ M BR trapped in a 1:1 OligAPol/FAPol_{AF647} mixture or with 1- μ M tOmpA trapped in a 1:1 OligAPol/A8-35 mixture, and then incubated for 1 h with 20 nM of a BR-specific antibody labeled with Alexa Fluor 488 or a tOmpA-specific antibody labeled with Alexa Fluor 647, respectively. NPs were then incubated with PPB-T20 for 10 min to wash off any non-specifically bound antibody and imaged.

Two different control experiments were designed to confirm the specificity of the interaction between Au NPs functionalized with cODN and OligAPol-trapped MPs: (i) Au NPs were incubated first for 2 h with 100 μ l of 1- μ M thiolated polycytosine DNA strands, which are not complementary to the ODN, and then with 1- μ M BR trapped in OligAPol/FAPol_{AF647}; (ii) Au NPs functionalized with the cODN were incubated first for 2 h with 2- μ M ODN labeled with a Cy3 dye and then for 2 h with BR trapped in OligAPol/FAPol_{AF647}. In both experiments, the samples were finally incubated for 10 min with PPB-T20 in order to remove any non-specifically bound protein.

The reversibility of the hybridization of the OligAPol to the cODN was investigated by first functionalizing Au NPs with cODN and BR trapped in OligAPol/FAPol_{AF647}, and then incubating the sample either with 8-M urea for 10 min under shaking or at 72°C in PPB for 10 min. The samples were then washed for 10 min with PPB-T20 and imaged in PPB.

RESULTS

Synthesis of OligAPol

Coupling reaction. OligAPol was obtained by forming an amide bond between an aminated ODN and one of the activated carboxylate functions of A8-35. The reaction was carried out in aqueous medium because of the low solubility of the ODN into organic solvent. This route has been used previously for the synthesis of sulfonated APols (24). Given that MP/A8-35 complexes typically comprise \geq 40-kDa APol per complex [reviewed in (2)], i.e. at least the equivalent of one A8-35 particle (10), a grafting level of at least one ODN per particle was aimed for, so as to ensure a nearly quantitative immobilization of any target MP.

Grafting is carried out in aqueous solution, i.e. on already assembled A8-35 particles. The synthesis protocol involves, first, the activation of free carboxylate groups of A8-35 by converting a fraction of them, in the presence of EDC and NHS, into a reactive NHS ester. The second step is the reaction of the ODN derivative with the activated ester function (Scheme 1). As observed in earlier works (25,26), determining optimum experimental conditions called for carrying out numerous preliminary tests in different aqueous and dimethylformamide (DMF)/H₂O buffers, at various ionic strengths (0.1–0.4 M NaCl), and for various ODN/A8-35 ratios and crosslinker concentrations (see the Materials and Methods section).

Monitoring OligAPol synthesis by SEC. A8-35 particles and the ODN used here have quite different masses (~40 and 6.6 kDa, respectively) and different spectroscopic properties [ODNs absorb maximally at 260 nm, whereas A8-35 is detected at 220 nm and does not absorb significantly at 260 nm; (3)]. SEC coupled with detection at multiple wavelengths is therefore an efficient way of following the conjugation reaction. Figure 1 shows the evolution of the chromatograms observed at 220 and 260 nm between the beginning of a synthesis, at $t = 0$ [i.e. before addition of EDC and NHS; panel (A)], and its end, at $t = 48$ h [panel (B)]. At $t = 0$, two peaks are observed. Peak ①, eluting at ~13.8 ml and absorbing both at 220 and 260 nm, corresponds to the free ODN, peak ②, eluting at ~12 ml and absorbing only at 220 nm, to A8-35 particles. After the reaction [panel (B)], the surface of the ODN peak decreases, while the A8-35 peak shifts to a lower elution volume (11.3 ml; peak ③), with the appearance of an absorbance at 260 nm and an increase of that at 220 nm, reflecting the grafting of the ODN. NHS elutes at ~17.5 ml [peak ④, panels (B) and (C)], traces of EDC at ~19 ml. OligAPol particles thus migrate as though they are significantly larger than those of ungrafted A8-35, and they seem more polydisperse. The decrease of the free ODN peak (①) at 260 nm provides an estimate of the evolution of the reaction, well correlated (within $\pm 20\%$) with the increase of the OligAPol one (③).

OligAPol purification. A two-step purification process was used to remove by-products and unreacted materials. Whereas free ODN remains water-soluble until pH \approx 2–3, A8-35 forms aggregates at pH < 7 and precipitates at pH < 5 (10,13). The first purification step therefore comprised

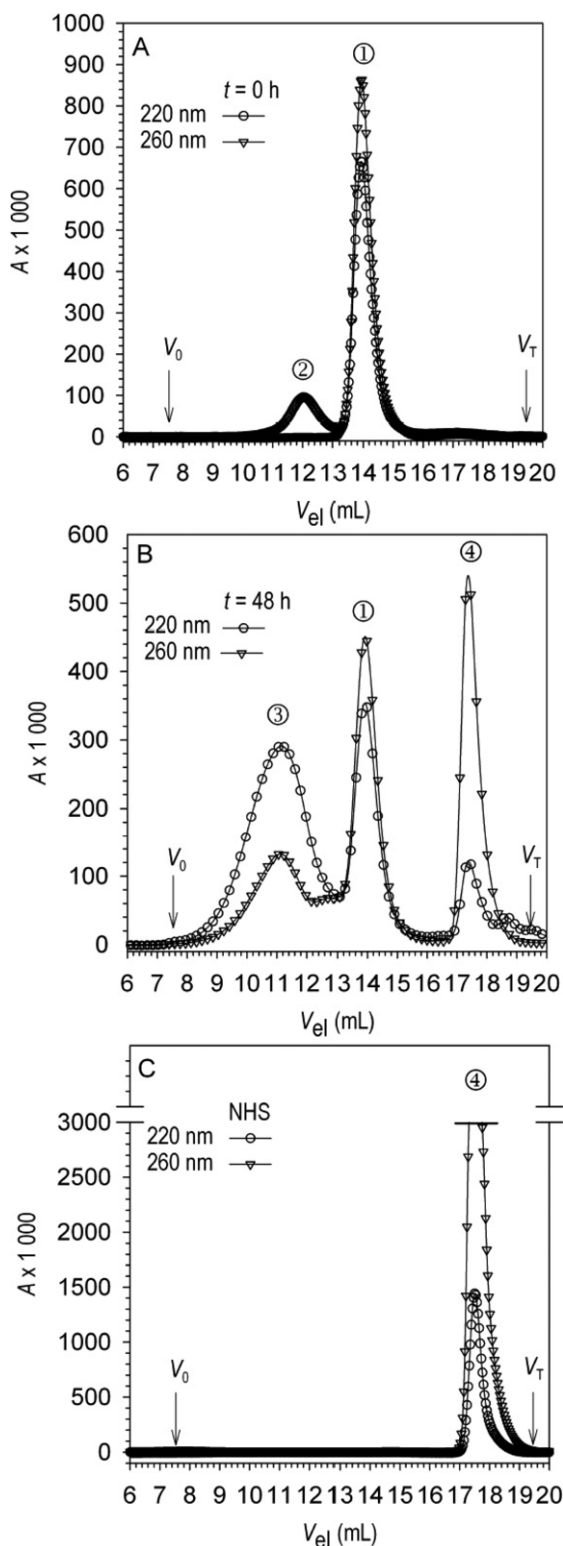


Figure 1. Monitoring of the coupling of ODN to A8–35 by size exclusion chromatography. Elution profiles at 220 nm and 260 nm of the reaction medium before [panel (A), $t = 0$] and 48 h after addition of EDC and NHS [panel (B)]. Initial concentrations were 13.2-g/l A8–35, 4.8-g/l ODN, 25.5-g/l EDC, 4.7-g/l NHS and 0.4-M NaCl. Panel (C) illustrates the elution of a 9-g/l NHS solution. Peaks are numbered as follows: ①, free ODN; ②, A8–35 particles; ③, OligAPol particles; ④, NHS. V_{el} , elution volume; V_0 , excluded volume; V_T , total volume.

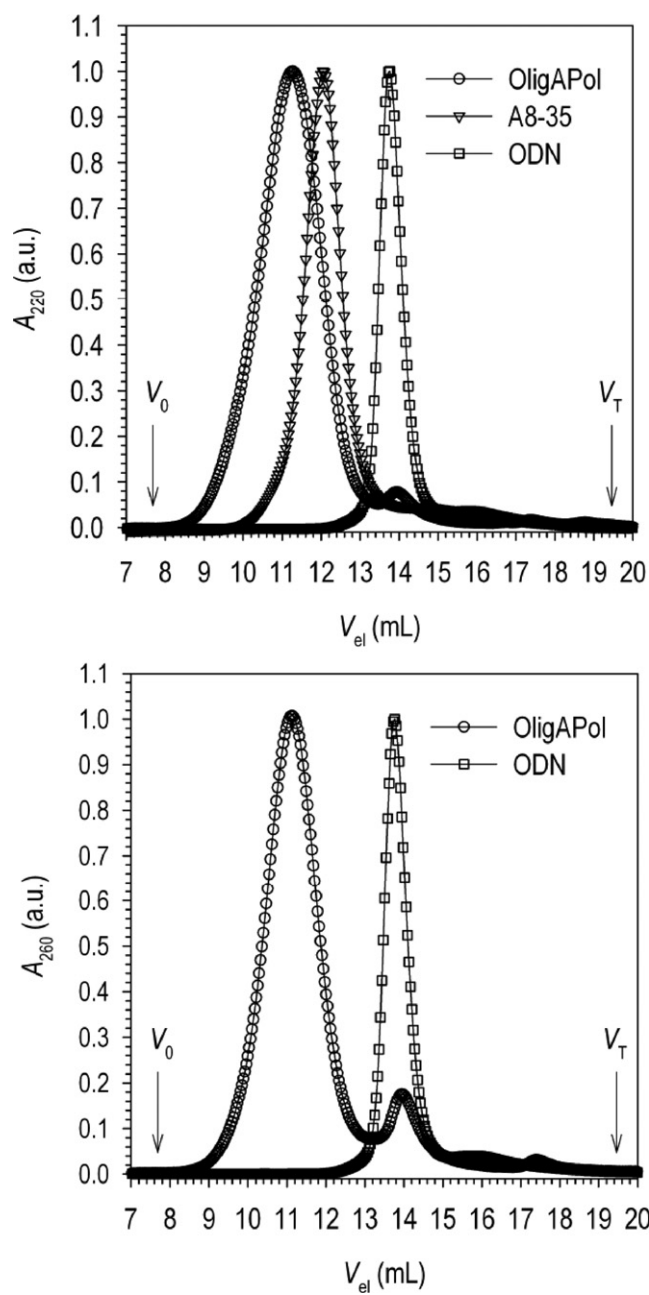


Figure 2. SEC analysis of purified OligAPol. Elution profiles at 220 nm (top) and 260 nm (bottom) of purified OligAPol and its precursors, A8–35 and ODN. The concentrations injected were ~4.9-g/l OligAPol, ~5.8-g/l A8–35 (~1.35 mM) and ~0.5-g/l (~0.076 mM) ODN. The profiles were normalized to the same maximum. a.u.: arbitrary units. V_{el} , elution volume; V_0 , excluded volume; V_T , total volume.

a selective precipitation at pH 3.25. Purification was incomplete, and most of the residual free ODN was removed by preparative SEC (see the Materials and Methods section).

For SEC characterization of the final product, stock solutions of ODN, OligAPol and A8–35 were injected onto a Superose 12 10/300 GL column (see the Materials and Methods section). Elution profiles with the absorbance at 220 and 260 nm normalized to the same maximum are shown in Figure 2. The peak of purified OligAPol is characterized by a

lower elution volume ($V_{el} = 11.3$ versus 12.0 ml) and a larger width at half height (W_{HH} = 1.8 versus 1.1 ml at 220 nm) than that of the precursor A8–35 (Figure 2, top). It appears narrower at 260 nm (W_{HH} = 1.5 ml), because ungrafted A8–35 does not absorb at this wavelength (Figure 2, bottom). A small fraction of residual free ODN is detected at ~14 ml (see below).

Quantification of ODN grafting ratio in OligAPol. The grafting ratio was determined as follows. First, the total mass of ODN present in purified OligAPol samples, m_{ODN} , was determined, using a calibration curve for free ODN, from the absorbance at 260 nm. Second, SEC analysis (Figure 2) established that residual ungrafted ODN represents ~10% of this total. Third, the mass of A8–35, m_{A8-35} , was calculated by subtracting m_{ODN} from the total mass of the purified OligAPol sample, determined by weighing. The mass ratio of grafted ODN to A8–35 was then calculated as $(m_{ODN} \times 0.9)/m_{A8-35}$. Under optimal conditions, this yielded a ratio of 0.078 g ODN per g A8–35. Given the molecular mass of the ODN (6.56 kDa), this corresponds to ~0.47 g grafted ODN per 40-kDa A8–35 particle. Purified OligAPol therefore consists of an ~1:1 mixture of grafted and ungrafted APol particles. The desirable objective of one ODN per particle appears out of reach using the present synthesis procedure (see the Materials and Methods section).

MP trapping: comparison between A8–35 and OligAPol

MP trapping by OligAPol was tested using BR as a model protein. PM was purified from *Halobacterium salinarum*, solubilized in OTG, and BR was transferred to APols as described in (15,27). Parallel trapping experiments were carried out using OligAPol and its parent A8–35, at protein/APol mass ratios varying from 1:2 to 1:10. After adsorption of OTG onto Bio-Beads and centrifugation, visual observation of the different samples showed that: (i) BR precipitated when OTG was removed in the absence of APol (negative control); (ii) a pellet was observed at BR/OligAPol mass ratios of 1:2 (important) and 1:5 (negligible); (iii) all of BR remained in the supernatant for the positive control (no removal of OTG, no APol), for BR/A8–35 samples at mass ratios 1:5 and 1:10 and for BR/OligAPol samples at mass ratios 1:7.5 and 1:10 (Figure 3, top). These results were confirmed by the UV-visible absorbance spectra of the supernatants, which showed the presence of native BR with a visible absorption peak at 554 nm (Figure 3, bottom), indicating that OligAPol keeps BR in its native state [upon denaturation, BR releases its cofactor, retinal, which absorbs at ~380 nm, as visible in the spectrum of sodium dodecyl sulphate (SDS)-denatured PM]. The percentage of BR kept soluble was calculated from the absorbance at 554 nm before and after ultracentrifugation (Figure 3, top). In the absence of surfactant, BR precipitated nearly quantitatively, whereas in the presence of OTG it remained soluble, a slight release of retinal—due to the lesser stability of BR in detergent solution—being responsible for the small peak observed at ~380 nm (Figure 3, bottom). At the lowest BR/OligAPol ratio used (1:2 w/w), ~70% of BR remained

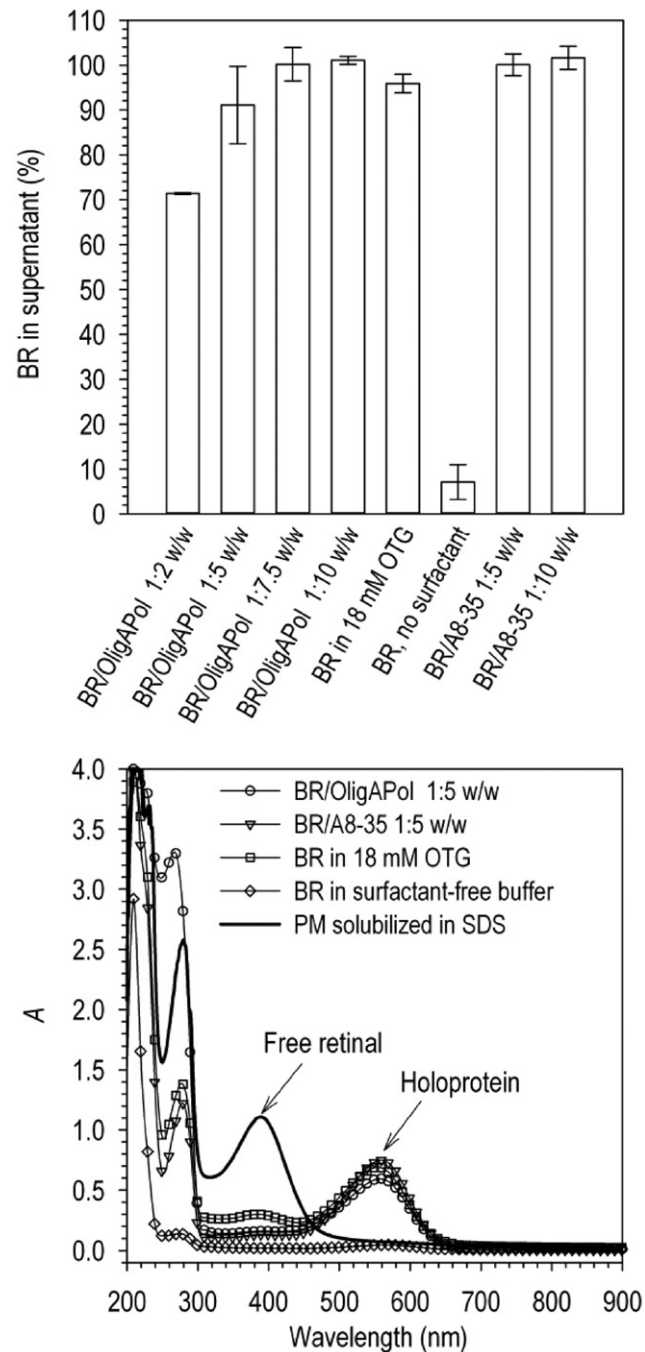


Figure 3. OligAPol keeps BR soluble and native. (Top) Percentage of BR present in the supernatant after trapping at BR/OligAPol mass ratios varying from 1:2 to 1:10. Absorbance at 554 nm was taken as a measurement of the concentration of native BR. Control samples included BR trapped in A8–35 at 1:5 and 1:10 mass ratios, BR kept in 18-mM OTG (positive control) and BR depleted from OTG in the absence of APol (negative control). Error bars correspond to the standard deviation on ≥ 3 experiments. (Bottom) To three identical samples of BR in OTG solution were added either OligAPol (○), or plain A8–35 (▽), both in a 1:5 BR/APol mass ratio, or no APol at all (◇). All samples were then depleted from OTG with Bio-Beads, except for the positive control (□). After overnight incubation at 4°C, the beads were removed and the samples centrifuged at 100 000 \times g for 20 min at 4°C before recording UV-visible absorbance spectra. The spectrum of SDS-solubilized purple membrane (solid line) shows the peak of absorbance at ~380 nm of free retinal released upon BR denaturation. V_{el} , elution volume; V_0 , excluded volume; V_T , total volume.

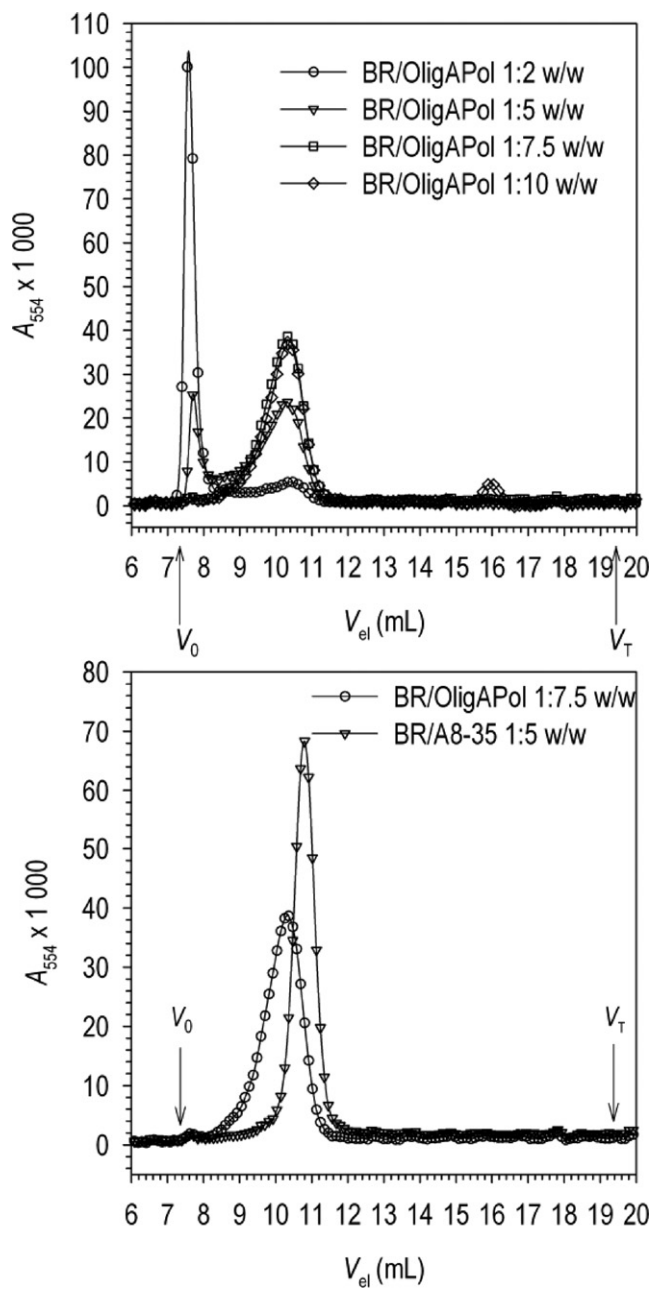


Figure 4. Size exclusion chromatography analysis of BR/OligAPol complexes and comparison with BR/A8-35 complexes. (Top) Chromatographic profiles at 554 nm of four BR samples trapped with OligAPol at BR/OligAPol mass ratios varying from 1:2 to 1:10. (Bottom) Chromatographic profiles at 554 nm of a sample of BR trapped at a BR/OligAPol mass ratio of 1:7.5 and a sample trapped in A8-35 at a BR/A8-35 mass ratio of 1:5. V_{el} , elution volume; V_0 , excluded volume; V_T , total volume.

in the supernatant; at all other ratios, the protein was completely soluble.

Supernatants were analyzed by SEC to estimate the size distribution of BR/OligAPol complexes. Figure 4 (top) shows the elution profiles at 554 nm for BR/OligAPol mass ratios varying from 1:2 to 1:10. At ratio 1:2, an important fraction of the protein was aggregated and eluted in the void volume V_0 of the column. At ratio 1:5, this fraction was

much reduced. At ratios 1:7.5 and 1:10 (Figure 4, top), no aggregates were present and a well-defined peak of soluble BR was observed. BR/OligAPol complexes elute at $V_e \approx 10.4$ ml, as compared to 11.3 ml for pure OligAPol particles. Their apparent size is significantly larger than that of BR/A8-35 ones, which elute at $V_e \approx 10.8$ ml (Figure 4, bottom). The BR/OligAPol peak is also broader, with a WHH increase from 0.6 ml to 1.2 ml, reflecting the fact that some complexes carry one or more grafted ODN(s) while others do not. The ability of A8-35 to trap and keep soluble BR, however, does not appear to be significantly affected by the presence of the ODN.

Accessibility of the ODN tag to hybridization with a cODN

A 2-g/l OligAPol solution was supplemented with cODN at 0.25 g/l final concentration, corresponding to a 1:1.6 molar ratio of ODN to cODN. The chromatograms at $\lambda = 220$ nm of the OligAPol sample and the OligAPol + cODN one are shown in Figure 5 (top). As observed before (Figure 2), the OligAPol sample migrates as two peaks, a minor peak of free ODN at $V_e = 14.0$ ml (labeled ① in the figure) and a major, broad peak at 11.3 ml, comprising a mixture of ODN-carrying and ODN-free A8-35 particles (②). The chromatogram of the mixture of OligAPol and cODN features four peaks: ①: a large peak at 14.1 ml, corresponding to the excess of cODN; ②: a small peak at 12.9 ml, due to the formation of the free ODN/cODN duplex; ③: a peak of ODN-free A8-35 particles at ~ 11.7 ml (this peak indeed does not appear at $\lambda = 260$ nm; not shown); ④: a large peak at 10.6 ml, representing the hybrid OligAPol/cODN. Because hybridization increases the R_S of this last fraction as compared to that of pure OligAPol, it becomes more distinct from untagged A8-35 (③) than OligAPol is in the absence of cODN (cf. Figure 2, top).

Next, cODN was added to BR/OligAPol complexes trapped at a mass ratio of 1:7.5 (final concentrations: 0.4-g/l BR, 3-g/l OligAPol and 0.37-g/l cODN, corresponding to molar ratios of ~ 2.2 ODNs per BR and 1.6 cODNs per ODN). At $\lambda = 554$ nm (Figure 5, bottom), the peak of BR/OligAPol complexes is seen to elute slightly earlier in the presence than in the absence of cODN, V_e shifting from 10.4 to 10.0 ml. The distribution becomes more markedly asymmetrical, because the R_S of the BR/OligAPol/cODN complexes increases with respect to that of the BR/OligAPol ones, while that of the BR/A8-35 complexes does not change. As a result, WHH increases from 1.2 to 1.55 ml.

In summary, SEC analyses indicate that the ODN tag is accessible and free to hybridize with a cODN whether the OligAPol exists as free particles or is bound to an MP.

Immobilization of OligAPol-trapped MPs onto magnetic beads carrying a cODN

cODN-coated magnetic beads prepared by reductive amination (see the Materials and Methods section) were used to immobilize BR/OligAPol complexes. The beads were incubated with five types of samples (Figure 6): (i) polyT, an ODN with a base sequence non-complementary to the

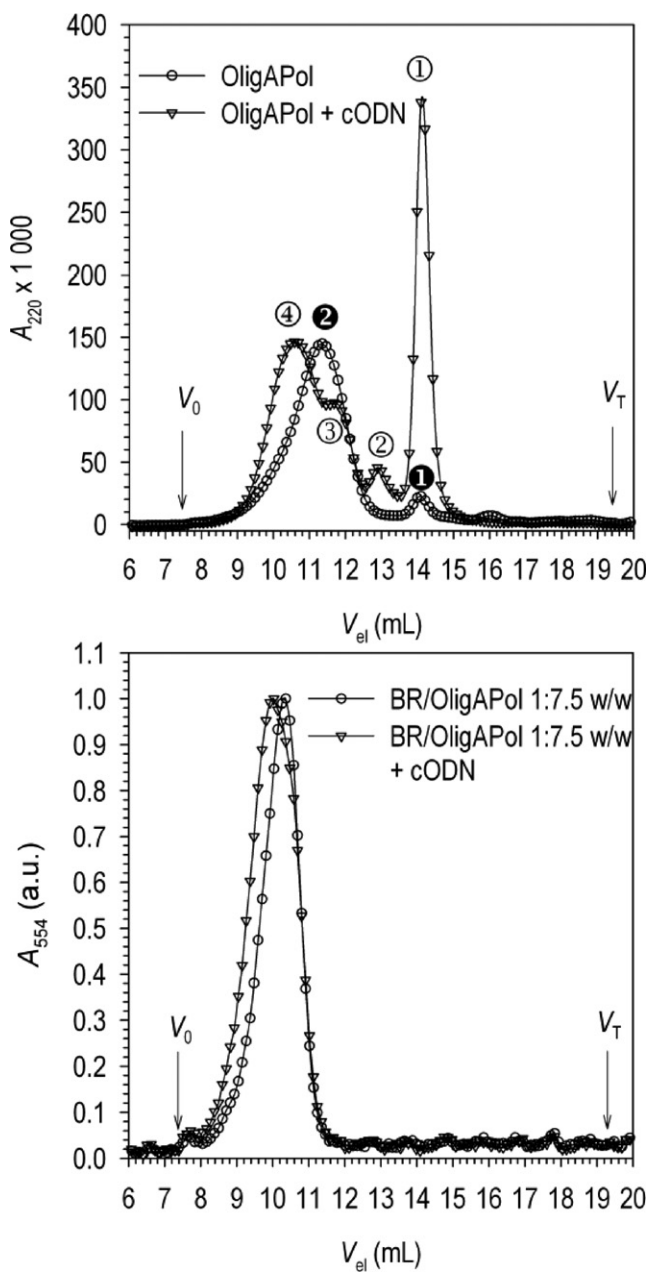


Figure 5. Accessibility of the ODN tag to hybridization with a cODN. (Top) Accessibility in OligAPol particles. Chromatograms at 220 nm of an OligAPol sample before (○) and after (▽) supplementation with cODN. (1) free ODN; (2) OligAPol particles; (3) free cODN; (4) ODN/cODN duplex; (5) ODN-free A8-35 particles; (6) OligAPol particles hybridized with cODN. (Bottom) Accessibility in BR/OligAPol complexes. BR was trapped at a 1:7.5 BR/OligAPol mass ratio and supplemented (▽) or not (○) with cODN. A_{554} absorbances were normalized to the same maximum. a.u.: arbitrary units. V_{el} , elution volume; V_0 , excluded volume; V_1 , total volume. The broadening of the peak of BR and its asymmetrical shape after addition of cODN reflect the fact that only approximately two-third of the BR/OligAPol complexes actually carry an ODN tag.

cODN; (ii) the ODN used to functionalize A8-35; (iii) unfunctionalized A8-35; (iv) free OligAPol particles; and (v) BR/OligAPol complexes. The degree of binding of each ligand to the beads was assessed by measuring the depletion of

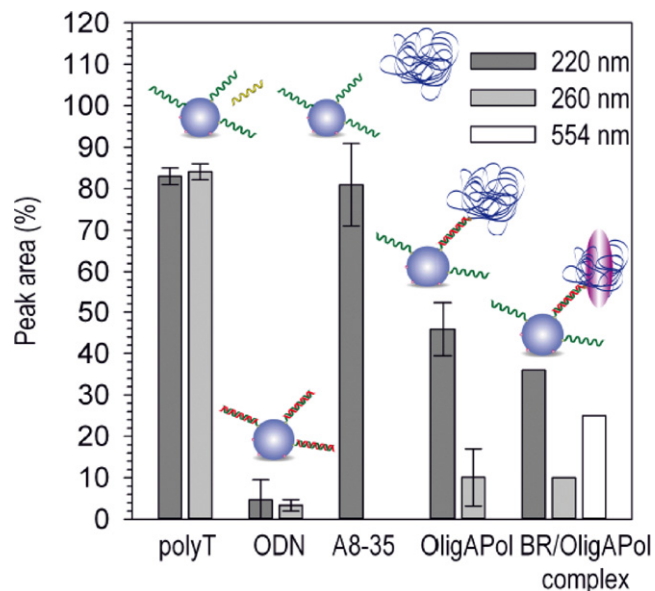


Figure 6. Quantitative analysis of the binding of ODN and OligAPol onto cODN-grafted magnetic beads. cODN-grafted beads (2 mg) were mixed with either polyT (0.05 mg), ODN (0.05 mg), A8-35 (0.25 mg), OligAPol (0.25 mg) or BR/OligAPol complexes (0.036-mg BR and 0.27-mg OligAPol). All samples except the BR/OligAPol one were incubated for 20 min at RT on a rotating wheel. To reach maximal adsorption, the BR/OligAPol sample had to be incubated for $2 \times \sim 15$ h at 4°C, with a renewal of the beads at mid-time (see text). The supernatants were subjected to SEC and the surface of the relevant peaks determined at 220, 260 and/or 554 nm. It is given as a percentage of that measured for an aliquot analyzed before the addition of the beads.

the sample by SEC. Very little interaction was observed in cases (i) and (iii), with more than 80% of the analyte (polyT or A8-35) remaining in the supernatant. On the contrary, free ODN (<10% of which remained in the supernatant), OligAPol and BR/OligAPol complexes hybridized specifically (Figure 6). In the case of pure OligAPol, <10% of the initial material was detected in the supernatant at 260 nm versus ~50% detected at 220 nm. This result was expected, given that OligAPol is an ~1:1 mixture of grafted and ungrafted A8-35 particles. Free ungrafted A8-35 particles, which absorb at 220 nm and virtually not at 260 nm, mostly remained in the supernatant, as observed for plain A8-35 [sample (iii)]. In the case of BR/OligAPol complexes, the absorbance of the sample dropped by >60% at 220 nm, a wavelength at which BR, the APol and the ODN all contribute, by ~90% at 260 nm, at which A8-35 essentially does not absorb, and by ~70% at 554 nm, where only native BR absorbs. These figures are consistent with expectations. BR has been shown to bind ~54 kDa of A8-35 per BR monomer (15). Given that the ODN grafting ratio in OligAPol is ~0.47 tag per 40 kDa, approximately two-third of the BR can be expected to actually carry at least one ODN tag, the rest being complexed by untagged A8-35. This is roughly consistent with the ~25% of BR that remain in the supernatant. On the contrary, nearly all of the ODN, whether free, bound to free OligAPol particles, or attached to BR/APol complexes, adsorbs onto the cODN-carrying beads. Presumably due to the lower temperature (4°C) and their larger size, MP/OligAPol complexes how-

ever adsorbed more slowly than OligAPol particles or free ODN, and reaching maximal adsorption required the addition of more beads (see the Materials and Methods section).

OligAPol-mediated immobilization of MPs onto gold surfaces

Au NPs immobilized onto PLL-modified glass slides were used to (i) explore the possibility of using OligAPol for anchoring MPs onto gold surfaces and (ii) directly observe, by fluorescence microscopy, the hybridization of MP/OligAPol complexes and cODN onto solid supports and the binding of antibodies to immobilized MPs. The strong electrostatic interaction between the positively charged PLL and the negatively charged surface of Au NPs ensured a stable immobilization. Differential interference contrast (DIC) images (Figure 7A) showed well-dispersed particles. After incubation first with cODN carrying a thiol tag, and then with ODN labeled with a Cy3 fluorescent tag, imaging showed co-localization of the DIC and fluorescence signals, indicating that Au-bound cODN retains its ability to hybridize to the ODN present in the soluble phase (Supplementary Figure S1).

To observe single beads carrying immobilized MPs, BR was trapped in a 1:1 mixture of OligAPol and Alexa Fluor 647-labeled A8–35 [FAPol_{AF647}; see (21)]. After incubation with these complexes, cODN-functionalized Au NPs exhibited a strong and homogeneous fluorescence signal (Figure 7B). Single-particle analysis of the fluorescence images showed a ratio between the average signal recorded on Au NPs and the background of ~10 (Figure 7G), indicative of a low level of non-specific binding of the mixed BR/OligAPol/FAPol_{AF647} complexes and free OligAPol/FAPol_{AF647} particles to the PEG silane layer. Similar results were obtained upon incubation of cODN-functionalized beads with another MP, tOmpA, trapped with the same 1:1 OligAPol/FAPol_{AF647} mixture (Supplementary Figure S2). The presence of the MPs onto Au NPs was confirmed by incubation with Alexa Fluor 488- or Alexa Fluor 647-labeled antibodies (16) directed against BR (Figure 7C) or against tOmpA (Supplementary Figure S3). Thus both BR and tOmpA, once anchored onto Au NPs via the OligAPol, retain their ability to recognize specific ligands.

Two different control experiments were designed to confirm the specificity of the interaction between cODN-coated Au NPs and OligAPol-trapped MPs. No binding was observed when Au NPs were coated with thiolated poly-cytosine, which is not complementary to the ODN (Figure 7E), nor onto cODN-coated Au NPs that had been preincubated with a free, Cy3-labeled ODN (Figure 7F), hybridization of the free ODN being confirmed by the fluorescence signal (Supplementary Figure S4). The specific signal measured in these control experiments was much lower (~10%) and barely emerged from the background noise (Figure 7G).

Reversibility of MP immobilization

Immobilization of MPs via OligAPols offers the advantage of being reversible. Supplementary Figure S5A

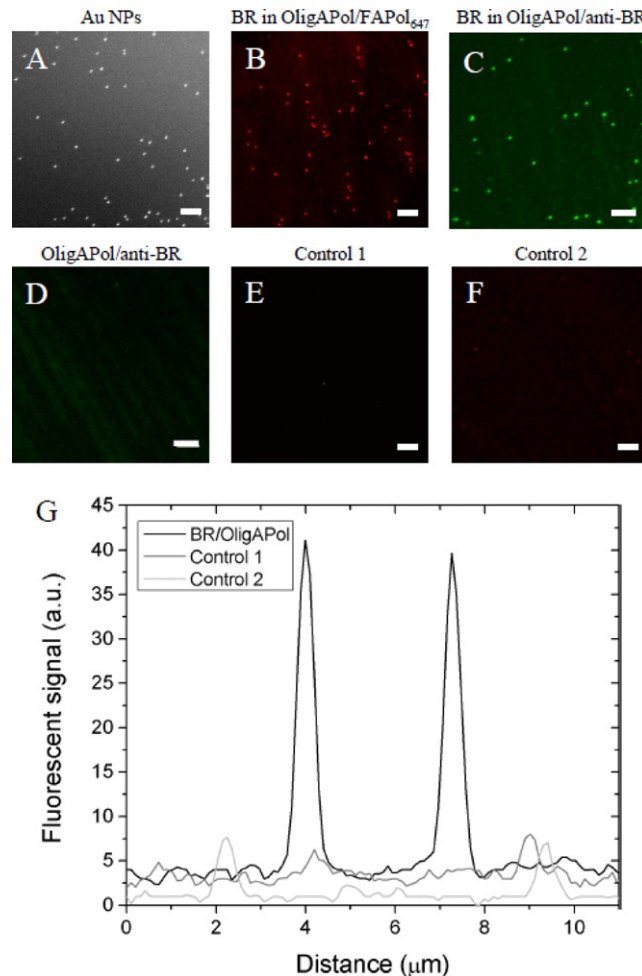


Figure 7. Immobilization of BR via OligAPol hybridization onto Au NPs and specific recognition by an anti-BR antibody. (A) DIC image of Au NPs (100-nm diameter) deposited on a PLL-modified glass slide and washed with 10-mM potassium phosphate buffer, pH 7.2 (PPB). (B) Fluorescence image of Au NPs preincubated with cODN, washed with PPB, and incubated for 2 h with BR trapped in a 1:1 OligAPol/FAPol_{AF647} mixture. (C) and (D) Fluorescence images of Au NPs preincubated with cODN, washed with PPB and incubated, for 2 h, either with BR trapped in a 1:1 OligAPol/FAPol_{AF647} mixture (C) or, as a control, with the OligAPol/FAPol_{AF647} mixture alone (D), after which both samples were washed with PPB and incubated for 1 h with a BR-specific antibody labeled with Alexa Fluor 488. The fluorescence image showed a much smaller signal when BR/OligAPol/FAPol_{AF647} complexes were incubated with particles coated with non-complementary poly-C DNA strands (E) or with Au NPs functionalized with the cODN, but hybridized with an excess of Cy3-labeled ODN prior to the addition of the BR/OligAPol/FAPol_{AF647} complexes (F). Brightness and contrast settings are the same for each set of images (B, E, F and C, D, respectively). Scale bar is 5 μm. (G) Line scans extracted from panels (B), (E) and (F). Each scan went through two representative NPs.

shows an image of Au NPs that were first functionalized with cODN and BR trapped in OligAPol/FAPol_{AF647}, and then exposed to urea. The fluorescence image (signal/background \approx 3) indicates that most of the complexes have been released from the Au surface. Similar results were obtained when cODN-coated Au NPs with bound BR/OligAPol/FAPol_{AF647} complexes were incubated above the estimated melting temperature of the

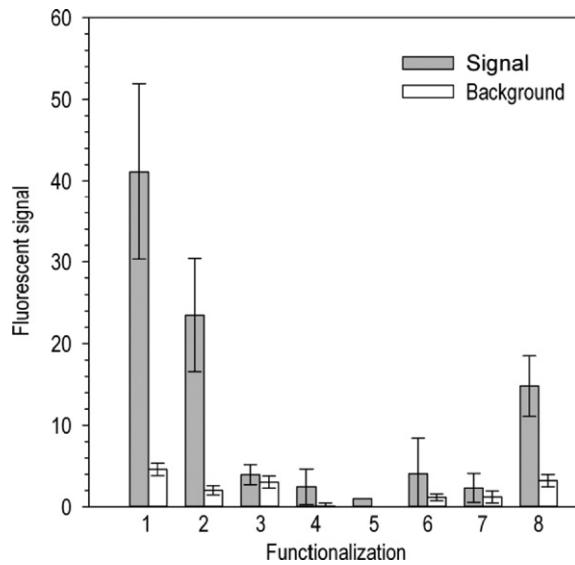


Figure 8. Average fluorescence signals measured on Au NPs following various treatments. **1.** Basic control for functionalization of Au NPs with the cODN: hybridization with an ODN labeled with a Cy3 dye. **2.** Immobilization onto cODN-coated NPs of BR/OligAPol/FAPol_{AF647} complexes. **3.** Control 1: Au NPs functionalized with poly-C, incubation with BR/OligAPol/FAPol_{AF647} complexes. **4.** Control 2: Au NPs functionalized with cODN and hybridized with an ODN labeled with a Cy3 dye before incubation with BR/OligAPol/FAPol_{AF647} complexes. **5.** Control 3: incubation of cODN-coated NPs with BR/A8-35/FAPol_{AF647} complexes. **6.** Dehybridization 1: incubation with 8-M urea of Au NPs with bound BR/OligAPol/FAPol_{AF647} complexes. **7.** Dehybridization 2: incubation at 72°C for 10 min of Au NPs with bound BR/OligAPol/FAPol_{AF647} complexes. **8.** Re-binding of BR/OligAPol/FAPol_{AF647} complexes to Au NPs that had been dehybridized for 10 min at 72°C.

duplex (Supplementary Figure S5B). The low residual fluorescence signal indicates that most of the BR/APol complexes have been released from the surface. cODN-coated Au NPs recover at least part of their binding capacity after the melting step: Au NPs re-incubated with BR/OligAPol/FAPol_{AF647} complexes showed a homogeneous fluorescence signal, demonstrating that complexes had bound again (Supplementary Figure S5C and D).

Quantitative fluorescence measurements on Au NPs under various conditions are summarized in Figure 8.

DISCUSSION

Synthesis of OligAPol

Under the present synthesis conditions, the grafting ratio of ODN to A8-35 approaches ~0.5 ODN per APol particle, which is less than what was aimed for but sufficient for the applications envisioned. Achieving higher degrees of tagging would require either a different grafting protocol or subsequent enrichment. The final preparation retains ~10% of unbound ODN. This, however, has only a marginal impact on MP immobilization.

Solution properties of OligAPol

A8-35 molecules (on average ~4.3 kDa) grafted with the ODN (6.6 kDa) assemble with ungrafted molecules to form

A8-35-like particles, indicating that the behavior of the polymer is not severely perturbed by the presence of the large hydrophilic tag. The hydrodynamic radii of OligAPol particles, A8-35 particles and free ODN are, respectively, ~4.1 nm, ~3.4 nm and ~2.1 nm (Figure 2). Most functionalized APols synthesized previously carried relatively small functional groups (5). Whenever examined, the size of APol particles was not affected, be it by the presence of NBD (7-nitrobenz-2-oxa-1,3-diazol-4-yle) (3), rhodamine (9), fluorescein (28) or biotin (unpublished data). Here, the ODN tag is big enough to detectably increase the R_S of OligAPol particles as compared to that of plain A8-35. This effect cannot be due to the increase in particle mass, which is negligible [~47 kDa with one ODN bound versus ~40 kDa for untagged particles (10)]. It suggests that the ODN extends away from the surface of the APol particle, possibly due to electrostatic repulsion. Nevertheless, the binding of such a large hydrophilic tag prevents neither the assembly of the polymer into well-behaved particles nor its use to trap MPs. This holds true, at least, for the present level of grafting.

MP trapping and hybridization

The ability of OligAPol to trap BR is similar to that observed for the precursor A8-35, but a slighter higher APol/protein mass ratio is required to ensure complete dispersion of BR into monomers. Considering that the particles are only ~8% more massive than those of plain A8-35 (on average ~43.3 versus ~40 kDa), one might have expected a negligible impact. Steric hindrance and repulsive interactions between ODN and A8-35 molecules may affect trapping efficiency. Yet, there is probably no redistribution of ODN-carrying molecules toward protein-free particles: indeed, the yield of immobilization of BR/OligAPol complexes onto cODN-bearing beads is consistent with a random distribution of grafted APols between free particles and protein-bound polymers, suggesting that there is no exclusion of the grafted polymers from the surface of the protein.

Immobilization of OligAPol-trapped MPs

OligAPol-mediated immobilization of MPs was demonstrated using two different MPs (BR and tOmpA), two different solid supports (magnetic beads and Au NPs), two methods for binding the cODN to the support (formation of a covalent bond or chemisorption) and two analytical techniques (spectroscopy and fluorescence microscopy), the ensemble of which provides complementary information on the yield of immobilization, its homogeneity, its reversibility and the generality of the approach.

Immobilization of free ODN and free OligAPol particles onto cODN-coated magnetic beads occurred rapidly (within 20 min at RT). The process was slower for BR/OligAPol complexes, requiring 2 × ~15 h (at 4°C), with a renewal of the beads at mid-time in order to reach maximal adsorption. This is probably due to slower diffusion at 4°C and a limited accessibility to the bead-bound cODN of the relatively large BR/OligAPol complexes (~95 kDa).

Fluorescence microscopy observation of the adsorption onto single Au NPs provided a more detailed view of the